Colliding Beam Fusion Reactor Space Propulsion System

A. Cheung,[1] M. Binderbauer,[2] F. Liu,[1]
A. Qerushi,[3] N. Rostoker,[3] and F. J. Wessel[3]

[1]*Department of Mechanical and Aerospace Engineering, University of California, Irvine, CA 92697-3975*
[2]*Tri Alpha Energy, Inc., 27211 Burbank, Foothill Ranch, CA 92610*
[3]*Department of Physics and Astronomy, University of California, Irvine, CA 92697-2225*
(949)824-3784, ahcheung@uci.edu

Abstract. The Colliding Beam Fusion Reactor Space Propulsion System, CBFR-SPS, is an aneutronic, magnetic-field-reversed configuration, fueled by an energetic-ion mixture of hydrogen and boron^{11} (H-B^{11}). Particle confinement and transport in the CBFR-SPS are classical, hence the system is scaleable. Fusion products are helium ions, α-particles, expelled axially out of the system. α-particles flowing in one direction are decelerated and their energy recovered to "power" the system; particles expelled in the opposite direction provide thrust. Since the fusion products are charged particles, the system does not require the use of a massive-radiation shield. This paper describes a 100 MW CBFR-SPS design, including estimates for the propulsion-system parameters and masses. Specific emphasis is placed on the design of a closed-cycle, Brayton-heat engine, consisting of heat-exchangers, turbo-alternator, compressor, and finned radiators.

CONCEPT DESCRIPTION

Exploration of the solar system (and beyond) requires propulsion capabilities that far exceed the best available chemical- or electric-propulsion systems (Stuhlinger, 1964). For advanced-propulsion applications the Field-Reversed Configuration, FRC, (Tuszewski, 1988 and Steinhauer, 1996) is a promising concept, providing: design simplicity, high-thrust, high-specific impulse, and high specific-power-density. An improved version of the FRC is the Colliding Beam Fusion Reactor, CBFR, where the ion temperature is 100's of keV and the size of the ion gyro-orbits is comparable to the radial dimension of the system.

The CBFR, first conceived by Rostoker, et al. (Rostoker, 1993 and 1997), provides a pathway for the use of advanced fuels, i.e., fuels that produce little or no radioactivity. Moreover, in a CBFR plasma confinement and transport are expected to be classical, based on Tokamak experiments involving energetic ions (Heidbrink, 1994). Analysis suggests that a CBFR could operate on a wide range of fusion fuels, i.e., D-D, D-T, D-He^3, H-B^{11}, H-Li^6, etc., and could scale over a wide range of output-power levels, from MWs to GWs (Rostoker, 2002).

A CBFR, fueled with H-B^{11}, is shown schematically in Figure 1. A super-conducting magnet provides the ambient-magnetic field. Energetic ion beams are injected tangentially (Wessel, 1990) into the fusion core to provide current drive and to re-fuel the reactor and the confined plasma has a large-angular velocity. The injected-ion velocities are the same, but their energies are different. A fusion reaction produces three, helium nuclei (i.e., α-particles), each with an average particle energy of 3.5 MeV. Since fusion products are produced isotropically in the plasma core, approximately half of the α-particles co-rotate with the fuel ions and the remaining half are counter-rotating. Surrounding the fusion-plasma core is a "magnetic separatrix" that defines the boundary between open and closed magnetic field lines. Plasma particles possessing non-resonant gyro-orbits diffuse rapidly to the separatrix and are expelled from the system, out both ends along magnetic-field lines.

CP699, *Space Technology and Applications International Forum–STAIF 2004,* edited by M.S. El-Genk

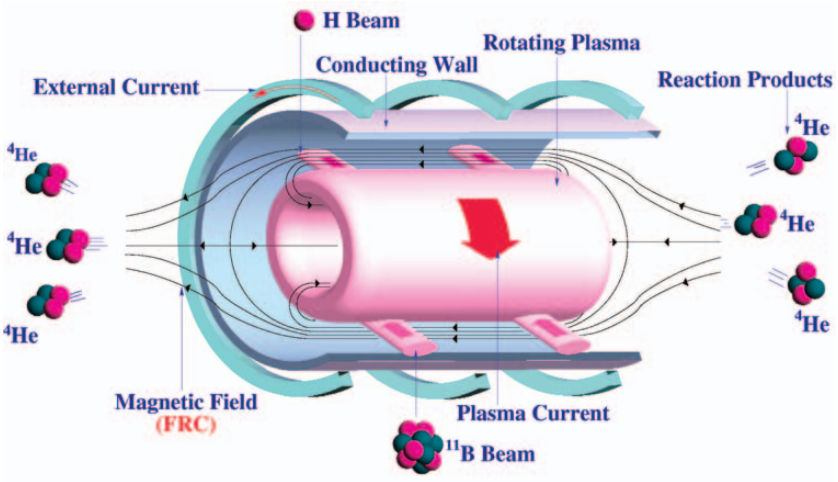

FIGURE 1. A Colliding Beam Fusion Reactor, CBFR, fueled with H-B^{11}.

The CBFR Space Propulsion System, CBFR-SPS, (Wessel, 2000) is illustrated schematically in Figure 2. A direct-energy converter intercepts approximately half of the α-particles, decelerates them by an inverse cyclotron process, and converts their kinetic energy into electric energy. A magnetic nozzle directs the remaining α-particles into space as thrust. Bremstrahlung radiation is converted into electric energy by a thermoelectric-energy converter, TEC. Bremstrahlung energy that is not converted by the TEC is passed to a Brayton-cycle heat engine. Waste heat is rejected to space. A power-control subsystem, not shown, monitors all sources and sinks of electric and heat energy to maintain system operation in the steady state and to provide an independent source of energy (i.e, fuel-cells, batteries, etc.) to initiate operation of the CBFR-SPS, from a non-operating state.

A system fueled by either D-T or D-He^3 is likely to be far more complex than what is shown in Figure 2. These fuel cycles produce a substantially higher fraction of their power output as energetic neutrons, hence their energy must be converted in a thermal cycle and thereafter, into thrust. Neutronic systems also require a massive radiation shield and support structure (Kammash, 1995 and Williams, 1997).

PERFORMANCE ESTIMATES FOR A 100 MW CBFR SPS

Table 1 summarizes the fusion-core parameters for a 100 MW CBFR module. A commonly used fusion power metric is the quality factor, $Q = P_N/P_R$, where P_N is the nuclear power and P_R is the radiated power. In the CBFR-SPS Q is highest for D-T, intermediate for D-He^3, and lowest for H-B^{11}. As the radial dimensions for all three systems are comparable, the reactor length needed for a 100 MW output is smallest for D-T, intermediate for D-He^3, and largest for H-B^{11}.

The CBFR-SPS specific impulse and thrust are shown in Table 2 and were estimated for each fuel cycle by considering all fusion product streams emanating from the core. All fuel cycles are assumed to use a magnetic nozzle that is 100% efficient.

H-B^{11} provides the highest thrust and thrust-to-power ratio, while D-He^3 is intermediate, and D-T is the lowest. The reduced thrust from a D-T system reflects the lower efficiency for converting a neutron product stream into a directed-energy flow. Whereas for D-He^3, where protons are the dominant components in the fusion-product stream, the net momentum per particle is less than for an equivalent power of α-particles, as produced by H-B^{11}. For a D-T system there are additional concerns related to material lifetime in the presence of a high-neutron flux, a closed thermal cycle that relies on the use of highly reactive and unstable liquid metals, and a need for a massive-radiation shield.

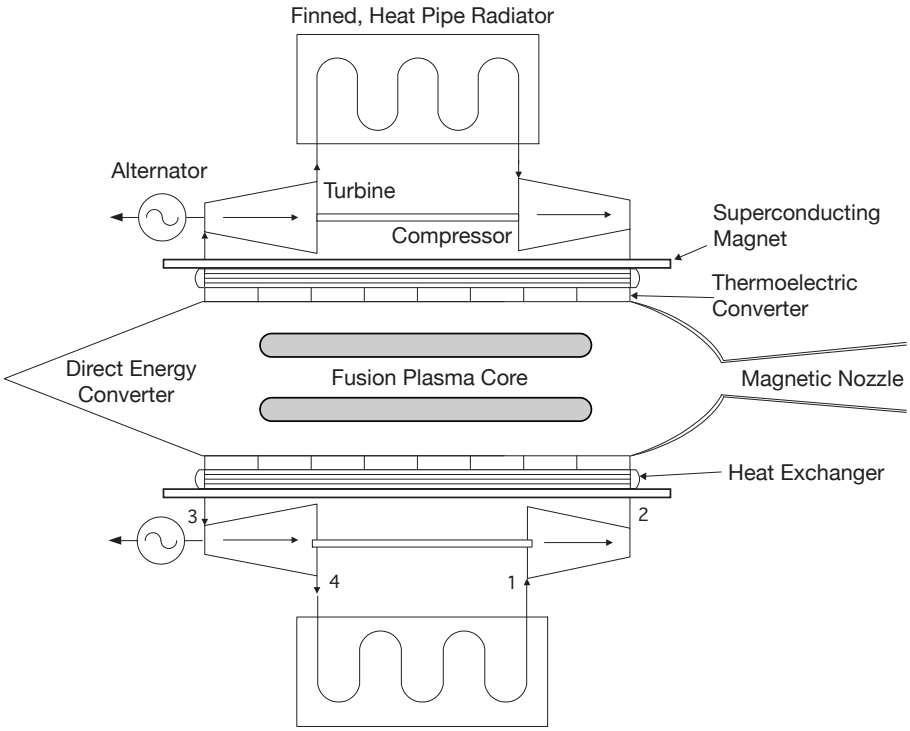

FIGURE 2. The Colliding Beam Fusion Reactor Space Propulsion System, CBFR-SPS.

MASS ESTIMATES FOR THE CBFR-SPS

The principal principal mass components in the CBFR-SPS are illustrated in Figure 3. The CBFR requires approximately 50 MW of injected power for steady-state operation. The H-B^{11} CBFR generates approximately 77 MW of nuclear (particle) power, half of which is recovered in the direct-energy converter with 90% efficiency. Thus, an additional 11.5 MW are needed to sustain the reactor which is provided by the thermo-electric converter and Brayton-heat engine.

The principal source of heat in the CBFR-SPS is due to Bremstrahlung radiation. The thermo-electric converter recovers approximately 20% of the radiation, or 4.6 MW, transferring approximately 18.2 MW to the closed-cycle, Brayton-heat engine. The Brayton-heat engine consists of a heat exchanger, turbo-alternator, compressor, and radiators, as shown in Figure 2. The Brayton engine supplies the remaining 7 MW of power needed sustain the reactor, another 11 MW is dumped directly to space.

A closed-cycle, Brayton-heat engine (Williams, 1997 and 2001) is a mature, and efficient option to convert excess heat rejected by the thermo-electric converter. In Brayton engines the maximum-cycle temperature is constrained by material considerations, which limits the maximum thermodynamic-cycle efficiency.

Consider the T-S diagram for the irreversible Brayton cycle, shown in Figure 4. The state points shown on the T-S diagram corresponds to the state points shown at the bottom of Figure 2. The heat source temperature is symbolized as T_H, while the heat sink temperature is symbolized as T_L. Processes $1-2_a$ (compression) and $3-4_a$ (expansion) are adiabatic, while processes 2-3 (heat addition) and 4-1 (heat rejection) are isobaric. Processes $1-2_s$ and $3-4_s$ presents the isentropic (ideal) operating scenarios, and differ because of turbo-machinery deficiencies. Subscripts 'a' and 's' refers to actual process and isentropic process, respectively.

The compressor and turbine efficiencies are, $\eta_c = (T_{2s} - T_1)/(T_{2a} - T_1)$, $\eta_t = (T_3 - T_{4a})/(T_3 - T_{4s})$. Compressor efficiencies can reach 85%, while turbine efficiencies can reach 90%. The counter-flow tube heat exchanger is assumed to have a 90% efficiency.

TABLE 1. Fusion Core Parameters for a 100 MW CBFR.

	D-T	D-He	H-B^{11}
Total Output Power, P_o (MW)	100	100	100
Fusion Energy/Reaction, E_F (MeV)	17.4	18.2	8.68
Densities $\times 10^{15}$ (cm^{-3}) ($n_e = 1$)			
n_1	0.5	0.33	0.5
n_2	0.5	0.33	0.1
Fuel Ion Energy (keV)			
$\frac{1}{2}\, m_1 V_1^2$	300	450	300
$\frac{1}{2}\, m_2 V_2^2$	450	675	3300
Temperatures (keV)			
T_i	96	217	235
T_e	100	170	85
Magnetic Field (kG)			
B_o	5.88	8.25	15.3
$B_o + B_m$	94.7	121	96.3
Nuclear (Particle) Power, P_N (MW)	99	84	77
Radiation Power, P_B (MW)	0.9	15.9	22.8
Recirculated Power, P_C (MW)	6.9	11.8	38
Nuclear Power/Radiation Power, $Q \equiv P_N/P_R$	112	5.28	3.84
Recirculated Power/Nuclear Power, P_C/P_N	0.07	0.14	0.49
(mean) PlasmaRadius, r (cm)	30	30	30
Plasma Width, Δr (cm)	3.8	6.8	10.3
First Wall Radius, R (m)	0.42	0.42	0.42
Chamber Wall Thickness, ΔR (m)	3.2	0.2	0.2
Chamber Length, L (m)	1.1	4.6	6.9
Chamber Volume, L (m^3)	45.3	5.6	8.3

TABLE 2. Propulsion Parameters for a 100 MW CBFR Space Propulsion System.

	D-T	D-He	H-B^{11}
Specific Impulse, $I_{sp} \times 10^6$ (s)	1.3	1.4	1.4
Thrust Power, P_T (MW)	29.9	67.8	50.8
Thrust Power/Total Output Power, P_T/P_o	0.3	0.68	0.51
Thrust, T (N)	3.8	9.6	28.1
Thrust/Total Output Power, T/P_o (mN/MW)	37.8	95.5	281

The heat load is transferred into the Brayton-engine from the cold-side of the thermo-electric converter: process 2_a-3. The hot and cold side heat exchanger heat conductance (product of heat transfer surface and heat transfer coefficient) are defined as U_H and U_L. The rate at which heat is transferred from the heat source to the cycle working fluid, and the rate at which heat is transferred from cycle to heat sink are: $Q_H = \dot{m}_{He} C_{p,He}(T_3 - T_2),\ Q_L = \dot{m}_{He} C_{p,He}(T_4 - T_1)$.

The effectiveness of heat exchangers are defined as: $E_H = 1 - e^{-N_H}, E_L = 1 - e^{-N_L}$, where N is the number of heat transfer units defined as: $N = U/\dot{m}C_p$. The thermodynamic efficiency of the cycle is defined as, $\eta = (Q_{in} - W_{out})/Q_{in} = 1 - (T_4 - T_1)/(T_3 - T_1)$ and the power output is defined as, $W_{out} = Q_H - Q_L$.

An ideal calculation benchmarks the performance. Isentropic compression and expansion are assumed; and turbo machineries are assumed to be 100% efficient. The hot-side heat exchanger, T_3, is calculated from knowing reactor core radiation temperature and thermoelectric converters efficiencies. From isentropic relations, maximum pressure ratios for a fixed T_3, and a design cycle calculation can be obtained.

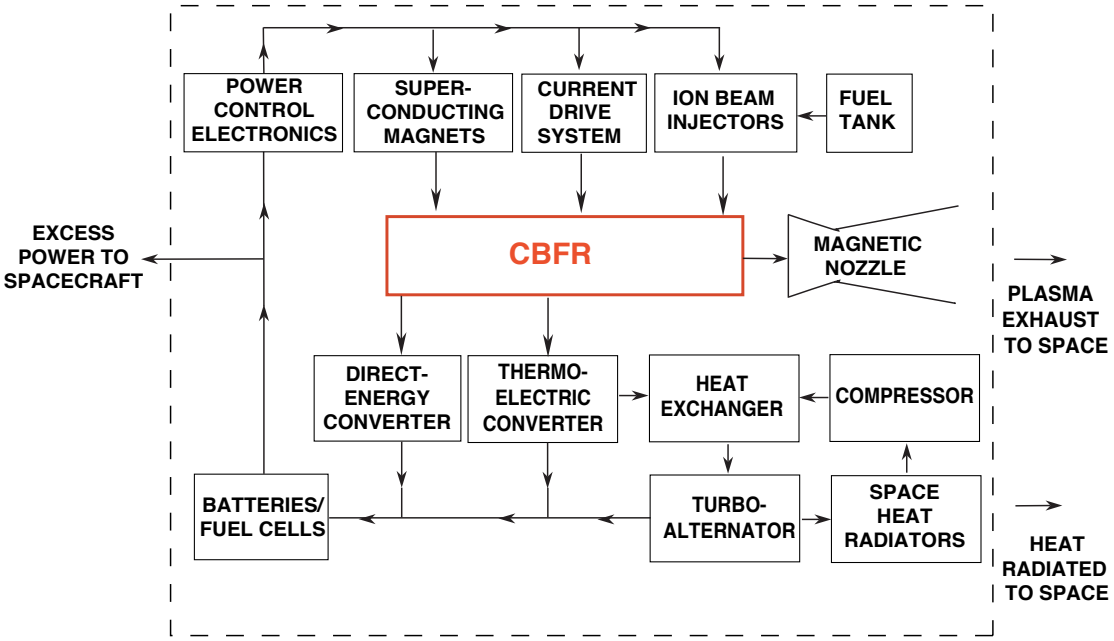

FIGURE 3. Block Diagram of the H-B^{11} CBFR SPS.

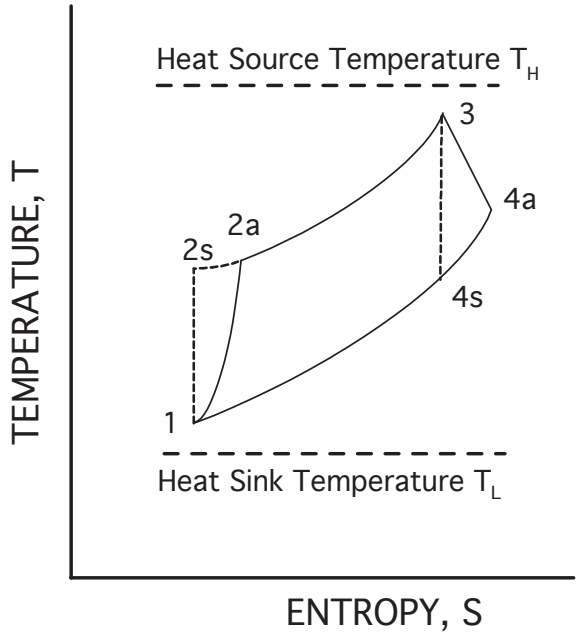

FIGURE 4. Temperature-Entropy Diagram for an Irreversible Brayton-Heat Engine.

A performance map for the Brayton engine is generated from the above equations. The results are shown in Figure 5 where the y-axis represents the thermodynamic efficiency and x-axis represents the hot-side temperature. The performance map shows the interaction between cycle pressure ratio and mass-flow rate. Since these two parameters determine the characteristics of the cycle, it is important to choose the correct combination. Because of peak-temperature constraints imposed on materials used in the heat exchanger and turbine, the right-side this performance is bounded to values less than 1675 ^{o}K, even though the thermal efficiency increases with temperature.

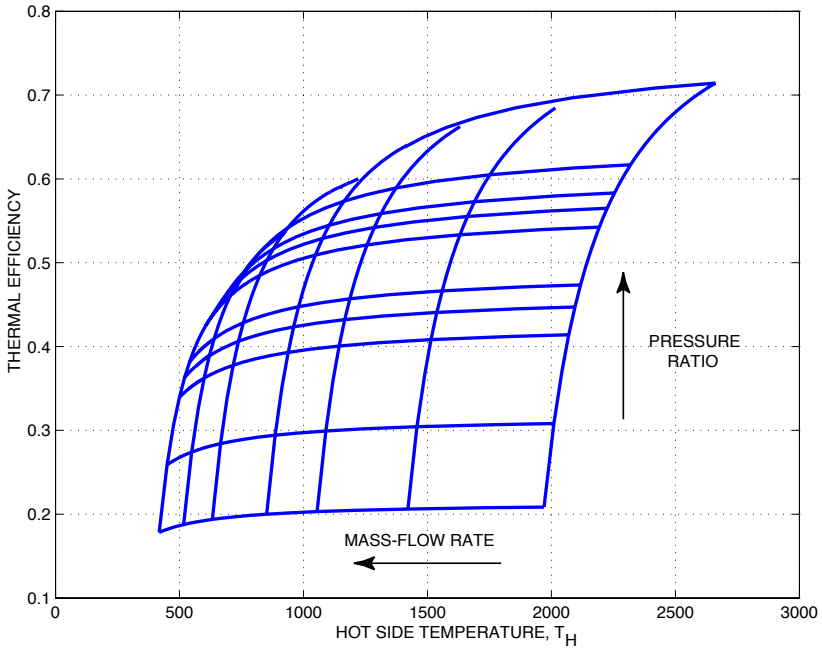

FIGURE 5. Efficiency-Temperature Diagram for an Irreversible Brayton-Heat Engine, with T_{min}= 100 K.

Based on the performance map, several design points are extracted. For a pressure ratio of 20, and cycle mass flow rate of 5 kg/s, the closed Brayton cycle can reach up to 60 per cent in thermal efficiency, recovering 16.3 MW out of 27.3 MW of waste energy. For the present case, we require 11 MW, hence, a 41 % efficiency is acceptable.

The component mass for the entire Brayton engine (less the heat radiators) is calculated based on specific-mass parameters typical of advanced industrial technologies, i.e, in the range of 3 kg/kW$_e$. Turbomachines, including compressors, power turbines, and heat exchangers, are combined for total mass of 18 MT.

The radiator mass is: $M_{radiator} = Q_{in}\kappa_R[1-\eta_c(T_{in}-T_{Rad})/T_{in}]/[\epsilon\sigma(T_{Rad}-T_{space})^4]$, where κ_R is material constant of radiator. T_{Rad} is the radiation temperature of the radiator, η_c is the overall conversion efficiency of the system (including turbomachineries and thermoelectic converters). The radiator mass is estimated to be 6 MT, using heat-pipe panels with state-of-the-art high thermal conductivity.

We have also estimated the total mass for the heat-rejection system as if it were entirely constructed of finned radiators and no Brayton-cycle heat engine. In this case the excess heat would be directly dumped to space with no energy recovery. For this case the mass of the radiators is approximately 35 MT.

The superconducting magnetic coils are made of Nb_3Sn, which operates stably at 4.5K and at a field up to 12.5 - 13.5 T. The cryogenic requirements for Nb_3Sn are less stringent than other materials considered. With a magnetic field of 7 Tesla and a device length of approximately 7.5 meters, the coil needs 1500 turns of wire carrying 56 kA of current. Using 0.5-cm radius wires, the total mass of this coil is about 3097 kg.

The liquid helium cooling system is comprised of two pumps, one at each end of the main coil. The total mass of these pumps is approximately 60 kg. The outer structural shell is used to support the magnets and all internal components from outside. It is made of 0.01-m thick kevlar/carbon-carbon composite with a total mass of about 772 kg. The outermost layer is the insulation jacket to shield the interior from the large temperature variation in space. The total mass is estimated to be 643 kg.

At present, the ion injection system most appropriate for space applications would be an induction linac or RFQ. Approximately 15 years ago an RFQ was flown on a scientific rocket and successfully demonstrated the use of high voltage power and the injection of ion beams into space. The design considered here is comprised of six injectors distributed along the length of the CBFR, three for each species of ion. Each injector is a 30 beamlet RFQ with an overall dimension of 0.3 meters long and a 0.020-m radius. Each injector requires an ion source, 0.02-meters long and 0.020-meters radius, that supplies ionized hydrogen or boron. One source is needed for each accelerator. Both the injector and the source are commercially available products; with design refinements for space their total mass, including the sources and the accelerators, should be 60 kg.

The cone-shaped direct-energy converter (DEC) is located at one end of the reactor, made of stainless steel, base radius, R = 0.49 meters and length, L = 2 meters. The DEC mass is approximately 1690 kg. An RF power supply (inverter/converter) recovers the directed-ion flow, converting it into electric power. The power supply mass is 30 kg. A storage battery is used to start/re-start the CBFR. The stored capacity is 30 MJ. It's mass is 500 kg. Alternately, a fuel cell could also be used. Additional control units coordinate the operations of all the components. The control-system mass is estimated to be 30 kg.

A magnetic nozzle is located at the other end of the CBFR SPS. The nozzle focuses the fusion product stream as a directed particle flow (Williams, 2001). At this time the design base for a magnetic nozzle is relatively undeveloped. Hence, we have assumed that the mass of the magnetic nozzle and the DEC are equal; since both are comprised of superconducting magnets and relatively low-mass, structural components.

The thermo-electric converter recovers energy from the electromagnetic emissions of the fusion core. It is a thin-film structure made of 0.02-cm thick boron-carbide/silicon-germanium, which has a mass density of about 5 g/cm^3. The TEC is located at the first wall and completely lines the inner surface of the reactor; the mass of the TEC is 400 kg. The radiant flux onto the TEC is 1.2 MW/m^2 and its peak operating temperature is assumed to be less than 1800 ^{o}K.

Using data from Tables 2 and 3 we obtain the following: total mass, $M_T = 32.97 \times 10^3$ kg, mass/total-power, $M/P_o = 0.33 \times 10^{-3}$ kg/W, and thrust/mass, $T/M_T = 0.85 \times 10^{-3}$ N/kg.

TABLE 3. Mass Breakdown for a 100 MW H-B^{11} CBFR SPS.

Brayton-cycle heat engine	18,000	
Finned Heat Radiators (Al composite,)	6,000	
Superconducting Magnet (Nb_3Sn)	3,097	
Direct Energy Converter (superconducting, SS inner/outer)	1,690	
Magnetic Nozzle (superconducting, SS inner/outer)	1,690	
Outer Structural Shell (composite)	772	
Outer Insulation Jacket (low density foam)	643	
Storage Battery (initial start-up)	500	
Thermoelectric Converter (BC/SiGe composite)	400	
Liquid He Recirculation/Cooling (15 kW)	60	
Ion Beam Injectors (3 each, for H and B^{11})	50	
RF Power Supply (converter/inverter)	30	
Feedback Control System Electronics	30	
Ion Source (bulk ionization)	10	
Total Mass	32,972	kg

CONCLUSION

The CBFR-SPS promises many benefits for advanced-space propulsion. Many of the technologies needed to realize a CBFR-SPS either exist, or could be developed readily in a several-year timeframe. Continued evolution and refinements in these technologies would favorably impact the definition of the CBFR-SPS concept reported here, for example: high-temperature superconductors, high energy density fuel cell technology, and advanced composite materials, etc. The scaleable nature of this system provides a cost-effective scenario for developing a flight system: development and testing could be done on a small, low-power device and then scaled up to a larger flight system. The use of H-B^{11} fuel would minimize the need for a large, massive, radiation shield. The high-beta, magnetic configuration and the use of energetic ions would facilitate the use of indigenous fuels, and perhaps enable system re-fueling at planetary destinations. Alternate design implementations of the CBFR-SPS could be used to provide prime power for existing, electric-propulsion concepts, for example: Hall thrusters, ion-propulsion systems, VASIMIR (Chang-Diaz, 1999), etc. The modular design of the CBFR-SPS could provide base-station power at a missions final destination, or to provide a staged approach to exploration, involving outpost-base stations.

REFERENCES

Chang Diaz, F. R. *Fusion Technology.*, **35**, p. 87, 1999.

Heidbrink, W. W. and Sadler, G. J., "The Behavior of Fast Ions in Tokamak Experiments," *Nuclear Fusion* **34**, p. 535, 1994.

Kammash, T., "Fusion Energy in Space Propulsion," *Progress in Astronautics and Aeronautics*, **167**, p. 1, 1995.

Rostoker, N., Wessel, F. J., Rahman, H. U., Maglich, B., Spivey, B., and Fisher, A., "Magnetic Fusion with High Energy Self-Colliding Ion Beams," *Physical Review Letters*, **70**, p. 1818, 1993.

Rostoker, N., Monkhorst, H., and Binderbauer, M. B., "Colliding Beam Fusion Reactor," *Science*, **21**, p. 1419, 1997.

Rostoker, N. and Qerushi, A., *Physics of Plasmas* 9, p. 3057, 2002.

Steinhauer, L., et. al, "FRC 2001: A White Paper on FRC Development in the Next Five Years," *Fusion Technology*, **30**, p. 116, 1996.

Stuhlinger, E., *Ion Propulsion for Space Flight*, McGraw-Hill, Inc., 1964.

Tuszewski, M., "Field Reversed Configurations," *Nuclear Fusion*, **28**, p. 2033, 1988.

Williams, C. H. and Borowski, S. K., "An Assessment of Fusion Space Propulsion Concepts and Desired Operating Parameters for Fast Solar System Travel," AIAA 97-3074, 1997.

Williams, C. H., Borowski, S. K., Dudzinski, L. A. and Juhaz, A. J., "Realizing 2001: A Space Odyssey," AIAA 2001-3805, 2001.

Wessel, F. J., Rostoker, N., Fisher, A., Rahman, H. U., and Song, J. J., "Propagation of Neutralized Plasma Beams," *Physics of Fluids*, **B2**, p. 1467, 1990.

Wessel, F. J., Rostoker, Binderbauer, M., and OToole, J. A., "Colliding Beam Fusion Space Propulsion System, *STAIF-2000*, American Institute of Physics 504, edited by Mohamed S. El-Genk, Albuquerque, NM, p. 1425-1430, 2000.